



Research article

Comparative evaluation of five extracellular vesicle isolation methods using proteomic profiling

Klara Mrazova^{1,2}, Tomas Henek¹, Zuzana Mihal Jurikova¹, Simona Koznarova³, Michaela Vasinova Galiova³, Jaromir Bacovsky⁴, Lenka Hernychova¹ and Roman Hrstka^{1,*}

¹ Research Centre for Applied Molecular Oncology (RECAMO), Masaryk Memorial Cancer Institute, Žlutý kopec 7, 656 53 Brno, Czech Republic

² Department of Biochemistry, Faculty of Science, Masaryk University, Kamenice 753/5, 625 00 Brno, Czech Republic

³ Institute of Chemistry and Technology of Environmental Protection, Faculty of Chemistry, Brno University of Technology, Purkyňova 118, 612 00 Brno, Czech Republic

⁴ DELONG INSTRUMENTS a.s., Palackého třída 153b, 612 00 Brno, Czech Republic

* **Correspondence:** Email: roman.hrstka@mou.cz; Tel: +420 543133306.

Abstract: Extracellular vesicles (EVs) research has gained a significant amount of attention in recent years. EVs are a heterogeneous group of different vesicles that vary in their origin, size, and function. The very nature of EVs, from their biogenesis to the contents of their cargo, offers many options for exploration. Despite being studied for a few decades now, there has not been an established standardized approach to isolation. However, the future use of EVs in clinical practice is conditioned by the optimization and standardization of isolation methods. In this study, we systematically compared common EV isolation techniques such as ultracentrifugation, precipitation, tangential flow filtration, and affinity-based methods using conditioned cell culture media as the source. Isolated EVs were analyzed using mass spectrometry to characterize their proteomic profiles, and the shared protein content was evaluated across datasets. The gene ontology enrichment was further assessed using three bioinformatics platforms. Among the tested methods, ultracentrifugation emerged as the most effective isolation method in our analysis, thus underscoring its importance among commonly used techniques. Despite its analytical robustness, this method is unsuitable for routine clinical workflows due to its complexity and time demands. Our findings highlight the need for a standardized, less strenuous EV isolation method for clinical applications.

Keywords: extracellular vesicles, isolation methods, comparison, mass spectrometry, proteomic analysis

Abbreviations: APOs: apoptotic bodies, BP: biological process, CC: cellular component, CCM: conditioned cell culture medium, DAVID: The Database for Annotation, Visualization and Integrated Discovery, DAVID Knowledgebase (v2023q4), DLS: Dynamic light scattering, EDS: energy-dispersive X-ray spectroscopy, EVs: extracellular vesicles, Exo: exosomes, ExoEasy: exoEasy Maxi Kit, FBS: fetal bovine serum, FunRich: Functional Enrichment Analysis tool version 3.1.4, GO: Gene Ontology knowledgebase version 2024-06-17, HCD: high-energy collision induced dissociation, LC-MS: liquid chromatography-mass spectrometry, MagCapture: MagCapture™ Exosome Isolation Kit PS Ver.2, MF: molecular function, MVs: microvesicles, PDI: polydispersity index, PEG: polyethylene glycol, SEC: size exclusion chromatography, TEM: Transmission electron microscopy, TEI: Total Exosome Isolation (from cell culture media) isolation kit, TFF: tangential flow filtration, Tim4: T-cell immunoglobulin domain and mucin domain-containing protein 4, UC: ultracentrifugation, XBP buffer: binding buffer, XE buffer: elution buffer, XWP buffer: wash buffer

1. Introduction

Cells release a variety of different extracellular vesicles (EVs) [1]. EVs are particles enclosed by a lipid bilayer, with a size of a few nanometers to 10 micrometers in diameter [2]. We recognize three main subgroups of EVs: microvesicles (MVs), apoptotic bodies (APOs), and exosomes, which differ from each other by their origin, biogenesis, and size [3]. MVs (50–1000 nm) emerge by directly budding from the plasma membrane [4], while apoptosis results in the extracellular release of APOs (50–2000 nm) [4,5].

Exosomes are EVs of endosomal origin with a size range of 30–150 nm [6,7]. The formation of exosomes occurs via plasma membrane inward budding [8]. Historically, exosomes were first identified as “platelet dust” [9]. In 1983, two papers [10,11] laid the foundation for further exosome research. Initially, exosomes were considered to collect cellular waste. Continued research has uncovered a wide range of biological functions for exosomes, along with a strong potential for diagnostic and therapeutic use [12].

Molecular composition and function are tightly connected. Even though this area of exosome research needs deeper investigations, the main biological functions with the involvement of exosomes are known. A frequently mentioned biological role of exosomes is intercellular communication [13]. Additionally, exosomes play an important part in cancer. They participate in the advancement of the disease on many levels [14], including metastasis [15], angiogenesis [16], gene expression regulation [17], and the alteration of immune responses [18]. In addition, they serve as carriers of diverse molecular biomarkers [19,20].

Exosomal cargo is heterogeneous with various types of proteins, lipids, and nucleic acids [21]. The proteome of exosomes is very diverse. Proteomic analyses have identified the presence of endosome-associated proteins (to name a few: annexins, flotillin, Rab GTPases, SNAREs, Alix, and TSG101) and proteins that belong to the family of tetraspanins. The presence of tetraspanins (CD63, CD81, CD9) [22] should be emphasized since they are typically found enriched in exosomes [23]. From the lipidomic point of view, exosomes are abundant in cholesterol, sphingomyelin, and

ceramides [24,25]. Moreover, the content of nucleic acids is diverse, including RNAs (e.g., mRNAs, miRNAs, small noncoding RNAs)[26] and DNA [27]. Additionally, the cargo of exosomes is affected by the type of cell that releases exosomes [28] and its physiological state [29].

Although EVs have been investigated for some time, the fully standardized process of EVs isolation has not been established yet [30]. The isolation process needs to be adjusted to the biological fluid, as its chemical and physical properties vary [31]. In the case of conditioned cell culture medium (CCM), knowing the detailed conditions in which cells were maintained is essential [32]. Additionally, prior to culturing, the use of fetal bovine serum (FBS) needs to be discussed with regard to the future use of isolated EVs. Culturing without FBS exposes cells to stress and changes their protein expression [33]. On the other hand, the use of EV-depleted media will still result in contamination by EVs originating in FBS [34].

Despite the progress in isolation and purification methods, reproducibility, sensitivity, specificity, and sample purity remain major issues [35]. Common isolation techniques are based on different properties of EVs (e.g., physical characteristics such as size and density or common EV markers). In a nutshell, used techniques mainly include ultracentrifugation, size-exclusion chromatography, precipitation, filtration, and affinity-based approaches [36,37]. Among all these methods, ultracentrifugation (UC) has led for many years, with 81% of scientists reporting using it for their isolation needs in 2015 [38]. Later, a similar survey found out that UC is still the most popular. Additionally, the survey also revealed the growing significance of size exclusion chromatography (SEC) [39].

Within this work, we present a comparative analysis of commonly used EV isolation techniques with a focus on the protein composition of the resulting vesicle preparations. To ensure that the evaluation reflects the major isolation principles applied in EV research, we selected five isolation approaches. SEC was not included in the present study, as SEC columns were not available at the time the experiments were performed. The protein content was assessed using liquid chromatography-mass spectrometry (LC-MS), thus enabling detailed proteomic profiling. Subsequent bioinformatic analyses identified a core set of proteins typically associated with EVs, thus providing insight into the consistency, specificity, and selectivity of each isolation technique.

2. Materials and methods

2.1. Cell cultures and collection of conditioned cell culture medium

Experiments were conducted using the human ovarian cancer cell line SK-OV-3 obtained from ATCC (American Type Culture Collection). For routine maintenance, the cells were cultured in McCoy's Medium (Sigma-Aldrich) containing 10% FBS (Biochrom), 20 mM L-glutamine (Gibco), and Penicillin-Streptomycin (10,000 units penicillin and 10 mg streptomycin per mL in 0.9% NaCl, Sigma-Aldrich) at 37 °C and 5% CO₂. The cells were grown to approximately 85–95% confluency before further treatment. Due to the natural presence of extracellular vesicles (EVs) in FBS, which could interfere with the experiments, the cells were maintained in a medium without FBS for 24 hours before medium collection. The samples were prepared in biological triplicates for each isolation experiment.

2.2. Techniques for EV isolation

To evaluate the impact of isolation methodology on the extracellular vesicle protein content, we applied five commonly used techniques: ultracentrifugation, tangential flow filtration, polymer-based precipitation, and two affinity-based methods. Each approach follows a distinct principle and varies in complexity, processing time, and specificity. A clear understanding of these differences is essential to choose the optimal method depending on the downstream applications. Figure 1 synoptically illustrates the step-by-step procedures involved in each protocol, highlighting both shared preprocessing steps and method-specific isolation workflows.

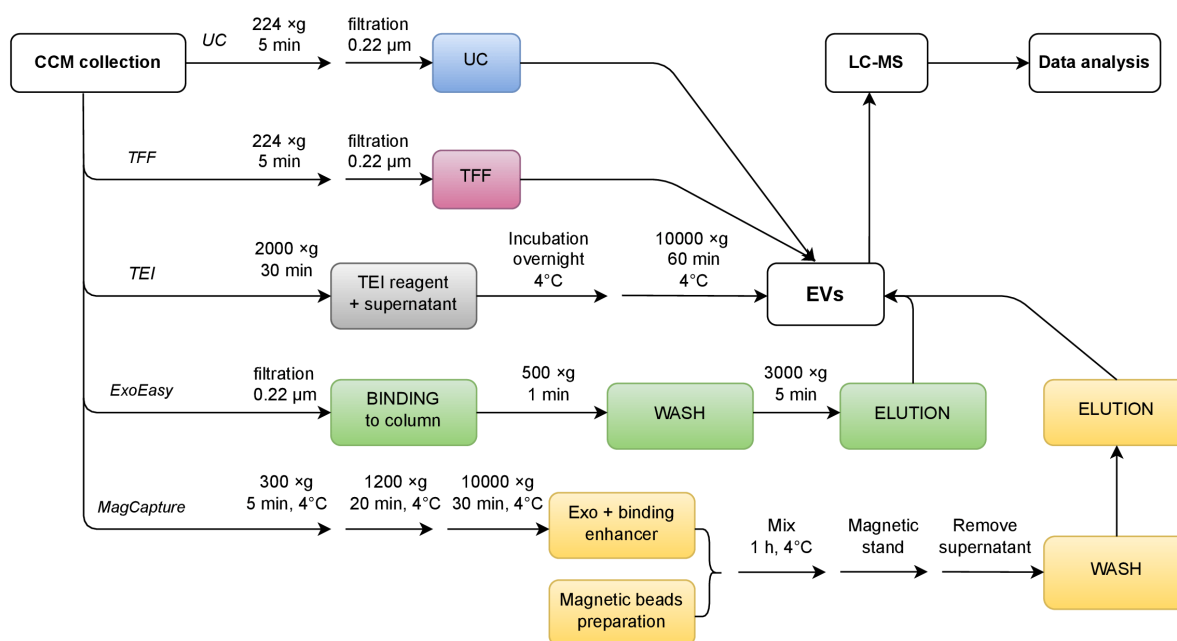


Figure 1. Strategies for EV isolation. The flow chart illustrates the procedures for each isolation approach used in this study. Samples were prepared in three biological replicates by each method (conditioned cell culture medium (CCM), ultracentrifugation (UC), tangential flow filtration (TFF), Total exosome isolation (TEI) (from cell culture media), exoEasy Maxi Kit (ExoEasy), MagCapture™ Exosome Isolation Kit PS Ver.2 (MagCapture), exosomes (Exo)).

2.2.1. Ultracentrifugation

The collected CCM was centrifuged ($224 \times g$, 5 min) and filtered through a $0.22 \mu\text{m}$ filter (TPP® Techno Plastic Products) to remove cellular debris and large EVs. Next, the CCM was centrifuged at $100,000 \times g$ for 90 min at 4°C (Beckman Coulter® Ultracentrifuge Optima XPN-80 Beckman Coulter, Rotor SW 32 Ti). After ultracentrifugation, the pellets were resuspended in $1\times$ PBS (137 mM NaCl, 2.68 mM KCl, 1.47 mM KH_2PO_4 , and 7.68 mM $\text{Na}_2\text{HPO}_4 \cdot 12\text{H}_2\text{O}$, pH 7.4) and stored at -80°C .

2.2.2. Tangential flow filtration

The isolation device tangential flow filtration (TFF)-easy (HansaBioMed Life Sciences, product code: HBM-TFF/1) works on a principle of TFF. The cartridge uses polysulfone hollow fibers with pores of 20 nm. First, the collected CCM was centrifuged ($224 \times g$, 5 min) and filtered through a $0.22 \mu\text{m}$ filter (TPP® Techno Plastic Products) to remove cellular debris and larger vesicles. The CCM was applied onto the cartridge using a syringe. Then, the EVs were concentrated in the retentate, while water and small molecules passed through the pores. The process of concentrating EVs is described in the protocol provided by the manufacturer. The EVs were recovered from the device using a syringe and stored ($-80 \text{ }^\circ\text{C}$) for future use.

2.2.3. Precipitation

The Total Exosome Isolation (from cell culture media) isolation kit (Invitrogen, cat. no. 4478359) was used to obtain the EVs by applying the precipitation principle. The process was carried out according to the manufacturer's instructions. Briefly, the collected CCM was centrifuged ($2,000 \times g$, 30 min). Next, 0.5 volumes of the Total Exosome Isolation (from cell culture media) reagent were added to the supernatant. The homogenous mixture was incubated at $4 \text{ }^\circ\text{C}$ overnight. Then, the samples were centrifuged ($10,000 \times g$, 60 min, $4 \text{ }^\circ\text{C}$) to prepare a pellet of EVs. The pellet was resuspended in $1 \times \text{PBS}$ and stored at $-80 \text{ }^\circ\text{C}$.

2.2.4. Affinity methods

EV isolation based on the affinity principle was carried out using the exoEasy Maxi Kit (Qiagen, cat. no. 76064). The kit contains columns with membranes on which EVs are retained. According to the manufacturer's recommendations, samples of the CCM were filtered ($0.22 \mu\text{m}$ filter). A mixture of binding buffer (XBP buffer) and CCM (1:1) was loaded onto the column. After centrifugation ($500 \times g$, 1 min), the EVs on the membrane were washed using wash buffer (XWP buffer) and again centrifuged ($3,000 \times g$, 5 min). In the end, an elution buffer (XE buffer) was used for EV elution. The eluate was collected after centrifugation ($500 \times g$, 5 min). The EV samples were stored at $-80 \text{ }^\circ\text{C}$.

EV isolation using the affinity principle was also tested by the MagCapture™ Exosome Isolation Kit PS Ver.2 (FUJIFILM Wako Pure Chemical Corporation, cat. no. 290-84103). EVs from the CCM were captured on magnetic beads through the interaction of proteins and metal ions with phosphatidylserine. After a series of washing steps using the buffer provided by the manufacturer, isolated EVs were released with the help of the elution buffer. The elution step was repeated twice, and the obtained EVs were stored at $-80 \text{ }^\circ\text{C}$.

2.3. Sample preparation for mass spectrometry

Samples prepared by various methods using different conditions were heterogenous, especially in terms of uneven volumes. In order to unify samples for LC-MS analysis, the samples first underwent evaporation using a vacuum concentrator (SpeedVac, Thermo Scientific™). The pellets were resuspended in $2 \times \text{Complete Sample Buffer}$ (13.6 mL distilled H_2O , 4 mL glycerol, 2.4 mL 1 M TRIS (pH 6.8), 0.8 mL 2% bromophenol blue in 1 M TRIS (pH 6.8), 4 mL 20% SDS, 10% mercaptoethanol),

and the volumes were empirically determined depending on the size of the pellet of each sample (30–300 μL). Short electrophoresis was performed with these samples (4–20% Mini-PROTEAN® TGX™ Precast Protein Gels, 120 V, 10 min). Afterwards, the gels were fixed in a solution of methanol and acetic acid for 15 min. The gels were incubated with Coomassie brilliant blue R250 for 30 min and then with a solution of methanol and acetic acid overnight to visualize the proteins (Appendix, Figure S1).

The gel pieces were washed with deionized water, cut into smaller pieces to facilitate buffer exchange, and decolorized with a freshly prepared 200 mM solution of ammonium hydrogen carbonate (NH_4HCO_3 , pH 7.8) in 40% (v/v) acetonitrile for 20 min at 30 °C and equilibrated in 50 mM NH_4HCO_3 (pH 7.8) in 5% (v/v) acetonitrile (equilibration buffer) for 30 min at 30 °C. The supernatant was removed, and the gel pieces were dehydrated with acetonitrile. The supernatant was removed, and the samples were reduced with 10 mM DTT for 1 h at 60 °C, followed by alkylation with 55 mM iodoacetamide in the dark for 45 min at room temperature. The supernatant was removed, and the gel pieces were washed three times with an equilibration buffer and dehydrated with acetonitrile. Trypsin digestion was carried out at 37 °C overnight using sequencing-grade trypsin (Promega, Madison, WI, USA). The digested peptides were extracted using acetonitrile, vacuum dried, and desalted using C18 micro spin columns (Harvard Apparatus) according to the manufacturer's guidelines. Briefly, the columns were equilibrated with a solution of acetonitrile and formic acid. The evaporated samples were dissolved in formic acid and loaded onto the columns. The follow-up procedure consisted of adding solutions of formic acid and acetonitrile. The step was repeated four times while the concentration of acetonitrile was increased in each step (20%, 30%, 40%, and finally 50%). Next, the samples were evaporated using a vacuum concentrator and dissolved in a solution of trifluoroacetic acid and acetonitrile (loading buffer).

2.4. Mass spectrometry

The LC–MS/MS analysis was carried out using an Orbitrap Fusion™ mass spectrometer (Thermo Fisher Scientific) with a New Objective digital PicoView 565 nanospray source (Scientific Instrument Services, Palmer, MA, USA) coupled to a Dionex™ UltiMate™ 3000 RSLC Nanoliquid chromatograph. Each sample injection contained approximately 200 ng per measurement, and the sample concentrations were determined using a NanoDrop spectrophotometer (Denovix DS-11+). The peptides were loaded into an Acclaim PepMap™ 100 nano trap column (nanoViper™ C18, 0.3 \times 5 mm, 5 μm particle size, 100 Å pore size; Thermo Fisher Scientific) with a loading buffer (2% ACN with 0.05% aqueous TFA (v/v)) for 5 min desalting at a flow rate of 5 $\mu\text{L}/\text{min}$. Next, the peptides were eluted onto an Acclaim PepMap™ RSLC C18 (nanoViper™ 75 μm \times 25 cm, 2 μm particle size, 100 Å pore size; Thermo Fisher Scientific) kept at 50 °C and separated by a linear gradient elution over 36-min from 2% to 25% B and a 5-min gradient from 25% to 60% B, followed by a 6-min wash step with 98% B, and 27 min of equilibration with 2% B. Mobile phase A was composed of LC–MS grade water and 0.1% formic acid (FA), while mobile phase B was 80% acetonitrile with 0.1% aqueous FA (v/v). The flow rate was 300 nL/min. The Orbitrap mass analyzer was operated in positive ion mode, with the static positive ion spray voltage set to 2.7 kV and the ion transfer tube temperature set to 275 °C. The master scan was acquired at resolving power settings of 120,000 (FWHM at m/z 200); the precursor mass range was 350–1400 m/z . The MS/MS spectra of multiply charged ions were collected in data-dependent mode (fragment and measure most intensive precursors for 2 s). Dynamic exclusion was set to 30 s. The peptides were fragmented using higher-energy collision induced dissociation

(HCD) with the normalized collision energy setting at 30% and the isolation window of 4 Da. The peptide fragments generated via HCD were detected in an ion trap (rapid scan rate). The mass spectra were analyzed using the Thermo Scientific™ Proteome Discoverer software, in which the MS PepSearch algorithm was employed to evaluate the spectra against the Consensus Human HCD Library (NIST). Spectra that were not assigned were subsequently processed using the Sequest HT search engine. For peptide identification and protein assignment, the UniProtKB/Swiss-Prot reviewed reference proteome (canonical sequences only; UniProt release 2023_05) was used; isoforms were excluded. To estimate and filter out false positive identifications, the Percolator algorithm was applied, maintaining the false discovery rate (FDR) below 1% at the peptide level. Some identified proteins were further annotated as contaminants based on their presence in the cRAP database (<https://thegpm.org/crap/>).

2.5. Data processing

Mass spectrometry provided lists of identified proteins for each sample. The samples were prepared in biological triplicates, so for each method there were three lists of proteins. First, proteins labeled as contaminants (by the software Thermo Scientific™ Proteome Discoverer) were eliminated, and the significant proteins were selected. A new dataset was prepared for every method consisting of proteins identified in all three samples for that method. Ergo, as a result, a total of five different datasets were analyzed.

A comparison of the datasets was facilitated by the Venn diagram generator (available on <https://www.biotoools.fr/misc/venny/>). The next steps of analysis were carried out using three different databases: The Database for Annotation, Visualization and Integrated Discovery, DAVID Knowledgebase (v2023q4) [40,41], Gene Ontology knowledgebase version 2024-06-17, 10.5281/zenodo.12173881 [42–44], and the FunRich Functional Enrichment Analysis tool version 3.1.4 [45]. Bioinformatic tools facilitated the term analysis to find terms linked to cellular components, molecular functions, and biological processes specific to our analyzed samples. Only terms with a p -value < 0.05 were considered relevant.

2.6. Characterization techniques

2.6.1. Western blot analysis

The EV samples were lysed in RIPA buffer (10 mM Tris-HCl (pH 7.4), 0.1% SDS, 1% sodium deoxycholate, 1% NP-40, and 152 mM NaCl) with added Halt™ Protease and Phosphatase Inhibitor Cocktail (100X) (Thermo Scientific™) (10 µL per 1 mL of RIPA) and shortly sonicated. Samples diluted with 4× Complete Sample Buffer (30% glycerol, 240 mM Tris-HCl (pH 6.8), 0.4% bromophenol blue, and 8% SDS) were loaded onto a 10% polyacrylamide gel. Equal volumes of EV samples with 4× Complete Sample Buffer (22 µL) from three biological triplicates were loaded per lane, while 15 µg of protein per lane was used for the SK-OV-3 cell lysate samples. The protein concentration of the cell lysate was determined using the Bradford assay. The protein concentration of the EV samples was not measured, as the objective was EV characterization rather than quantitative comparison, and the sensitivity of the Bradford assay was insufficient for the EV samples. Electrophoresis was performed in MOPS buffer (1 M MOPS; 1 M TRIS base; 70 mM SDS; 20 mM

EDTA) at 120 V for 1 h. The proteins were transferred from gels onto nitrocellulose membranes (0.2 μm pore size, BioTrace™) at 100 V for 90 min. The membranes were blocked in 5% skimmed milk at room temperature for an hour. The primary antibodies diluted in 3% BSA anti-CD9 (1:1000) (clone Ts9, ThermoFisher Scientific), anti-CD63 (1:1000) (clone Ts63, ThermoFisher Scientific, anti-CD81 (1:1000) (clone M38, ThermoFisher Scientific), and anti-calnexin (clone C5C9, Cell Signaling) were applied on membranes overnight at 4 °C. The membranes were washed four times in 1 \times PBS with 0.1% Tween and incubated with either goat or swine secondary antibodies conjugated with horseradish peroxidase diluted in 5% skimmed milk (1:1000) for 1 h at room temperature. The membranes were washed in the same manner as the day before. The enhanced chemiluminescence (ECL) detection reagent was prepared by mixing solutions A (200 mM TRIS, pH 9.4; 10 mM luminol, 405 mM p-coumaric acid; 0.5 mM EDTA, pH 8.0) and B (0.5 mM EDTA, 8 mM sodium perborate tetrahydrate, 50 mM sodium acetate, pH 5.0) in a 1:1 ratio immediately prior to use. The solution was applied to the membranes for 5 minutes. The chemiluminescent signals were detected using a G:BOX Chem XX6 imaging system (Syngene).

2.6.2. Dynamic light scattering (DLS)

The size measurement of the particles was performed by dynamic light scattering (DLS). The samples were loaded into a 2 Microlitre Quartz Cuvette (ZMV1002, Malvern Pananalytical Ltd). The particles were analyzed by Zetasizer μV (Malvern Pananalytical Ltd) under a 90° angle. The temperature was maintained at 25 °C during all measurements. Data acquisition was performed using the Zetasizer software, v7.11 (Malvern Panalytical Ltd). All samples were measured in technical triplicates. The analysis provided particle size distributions expressed as hydrodynamic diameter and polydispersity index (PDI) values.

2.6.3. Transmission electron microscopy

Imaging was performed using a low-voltage transmission electron microscope (LVEM25E; DeLong Instruments, Czech Republic). The microscope operates at an accelerating voltage of 25 kV, which provides enhanced image contrast due to the increased interaction between the electron beam and the specimen at low energies. This higher image contrast makes the LVEM25E particularly advantageous to image specimens composed of light elements, such as the EVs examined in this study.

The low-voltage operating conditions of the LVEM25E enable the efficient visualization of nanoscale biological structures, thereby providing sufficient contrast and structural detail of EVs. First, carbon-coated 300-mesh copper grids were coated by approximately 6–8 nm carbon film and glow-discharged for 10 seconds immediately prior to use. 10 μL of the sample was applied onto the grid and incubated for 30 seconds. The extra liquid was blotted off with filter paper. The grids were washed with double distilled water and blot dried with filter paper. Next, the EV samples were negatively stained using UA Zero, a uranyl acetate substitute that provides strong contrast while minimizing toxicity and handling concerns—10 μL of UAzero was applied onto the grid and incubated for 30 sec. The excess stain was blotted off with filter paper. The grids were let to completely air-dry before imaging.

3. Results

3.1. Protein counts

The analysis of isolated EVs by LC-MS/MS showed a different number of proteins for each sample. First, proteins labeled as contaminants by the Thermo Scientific™ Proteome Discoverer software were eliminated from the given dataset. The remaining proteins were termed ‘significant,’ as all subsequent analyses were based on this subset.

Figure 2 shows a comparison of the tested isolation methods, indicating that UC was the most efficient method, as it yielded the highest average number of identified proteins (543 proteins). In contrast, the lowest protein yield was observed in samples isolated by the MagCapture™ Exosome Isolation Kit PS Ver.2, with an average of 277 proteins. The analysis of contaminants revealed the poor performance of the TFF method, where samples processed with the hollow fiber cartridge contained the highest number of contaminants (average: 119). The ExoEasy kit produced samples with the lowest number of contaminants (average: 62 contaminants), narrowly outperforming the MagCapture kit (average: 67 contaminants).

If we were to assort the methods depending on the ratio of ‘significant proteins (average) vs. contaminants (average),’ the order of methods from highest to lowest would be as follows: UC (5.3) > ExoEasy (4.6) > MagCapture (4.1) > Total Exosome Isolation (from cell culture media) (3.9) > TFF-easy (2.8). According to this comparison, UC brought the best results.

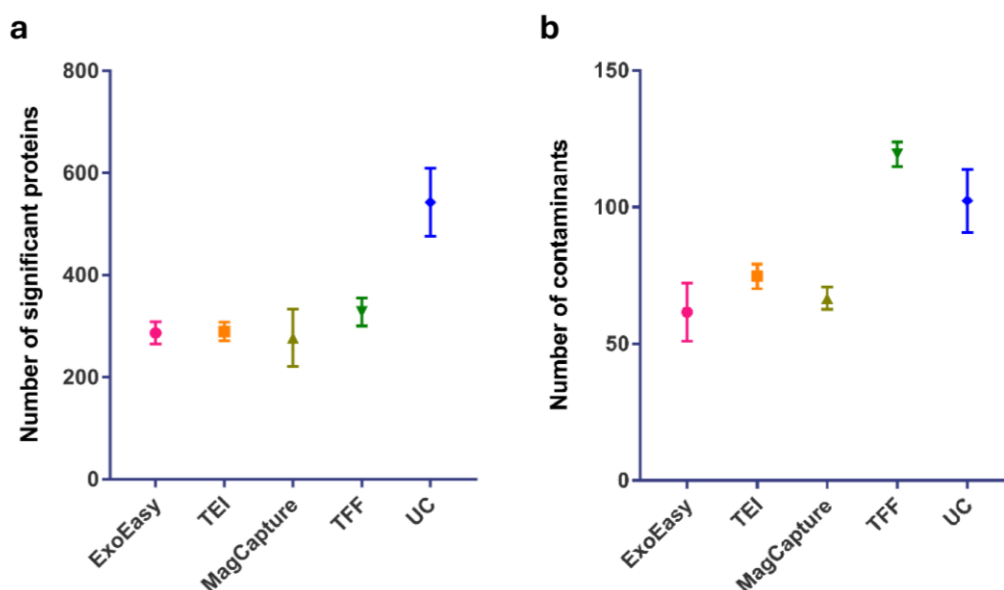


Figure 2. Evaluation of isolation methods. Comparison was based on (a) a number of detected significant proteins and (b) a number of detected contaminants (exoEasy Maxi Kit (ExoEasy), Total exosome isolation (TEI) (from cell culture media), MagCapture™ Exosome Isolation Kit PS Ver.2 (MagCapture), tangential flow filtration (TFF), ultracentrifugation (UC)).

3.2. Identification of common proteins

To identify proteins shared across all isolation methods, a selection of significant proteins was performed. Due to the variability in protein presence in each individual sample of a triplicate, only proteins consistently detected in all three replicates for each method were included in the analysis. Then, these refined datasets were compared. The analysis unveiled 61 common proteins (i.e., proteins that were identified by all methods in all samples). The result of the analysis is demonstrated in Figure 3. The simplified list of common proteins is provided in Appendix, Table S1. Comprehensive LC-MS/MS results for the 61 commonly identified proteins, including quantitative abundance information, are presented in Appendix.

The list of common proteins was compared with the top 100 proteins commonly identified in EVs, as listed in Vesiclepedia [46] using the FunRich Functional Enrichment Analysis tool version 3.1.4 [45]. Interestingly, the outcome showed 16 proteins in common (Table 1 and Appendix, Figure S2). This analysis confirmed that our significant proteins are associated with the EV cargo, as evidenced by Vesiclepedia. However, these findings suggest a potential contamination of the isolated EVs by lipoproteins and, possibly, cellular debris.

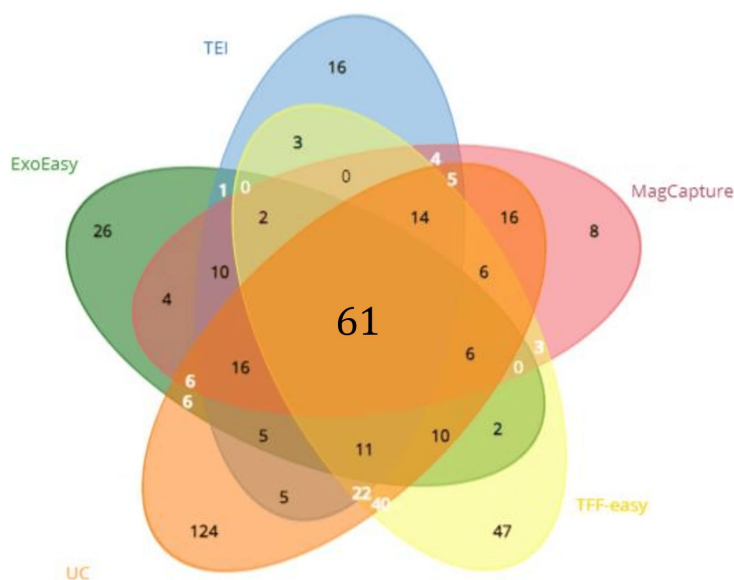


Figure 3. Overlaps of proteins identified by individual methods. The diagram was created using the Venn diagram tool available at <https://www.biotoools.fr/misc/venny/>.

Table 1. Overlapping proteins identified both in Vesiclepedia's Top 100 list and among the 61 common proteins detected in our study.

Gene symbol	Protein name
ANXA2	Annexin A2
ENO1	Alpha-enolase
HSPA8	Heat shock cognate 71 kDa protein
GAPDH	Glyceraldehyde-3-phosphate dehydrogenase
LDHA	L-lactate dehydrogenase A chain
EEF1A1	Elongation factor 1-alpha 1
A2M	Alpha-2-macroglobulin
CFL1	Cofilin-1
PKM	Pyruvate kinase PKM
ALDOA	Fructose-bisphosphate aldolase A
HSPA5	Endoplasmic reticulum chaperone BiP
FN1	Fibronectin
YWHAZ	14-3-3 protein zeta/delta
HSP90AB1	Heat shock protein HSP 90-beta
HSP90AA1	Heat shock protein HSP 90-alpha
MFGE8	Lactadherin

3.3. Comparative functional analysis across databases

The Database for Annotation, Visualization and Integrated Discovery, DAVID Knowledgebase (v2023q4) [40,41], Gene Ontology knowledgebase version 2024-06-17, 10.5281/zenodo.12173881 [42–44], and FunRich Functional Enrichment Analysis tool version 3.1.4 [45] were used to analyze the dataset of 61 common proteins. The main interest of this search was to recognize roles of identified proteins in biological processes and molecular functions, plus to reveal the relation of proteins to cellular components. Since there are differences between databases, we wanted to examine the terms on which they agree. Information was retrieved from each database and filtered by p-values. Only terms with a p -value < 0.05 were kept. Selected groups of terms (Cellular Component (CC), Biological Process (BP), and Molecular Function (MF)) from each database were compared using FunRich [45]. In other words, the most relevant terms for our set of proteins were gathered by each database, and then the relevancy was confirmed by comparing databases.

A comparison of the data acquired by the analysis focused on CCs confirmed the EV origin of given proteins. Results of all three databases included terms such as ‘extracellular exosome,’ ‘extracellular region,’ and ‘extracellular space,’ to name a few. The total number of common terms was 32. Similarly, the analysis of BPs revealed 46 common terms, including entries such as ‘cell adhesion,’ ‘protein folding,’ and ‘angiogenesis’. The MF analysis showed the involvement of proteins in various protein binding activities. Results of the comparison are summarized in Figure 4. The top ten results of a term analysis for each database are listed in Appendix, Figure S3. Overall, we conducted a term analysis focused on CCs, BPs, and MFs of identified common proteins. The outcome showed a link to EVs and components of a cell, while also enriching the analysis with insights into the specific functions of the proteins.

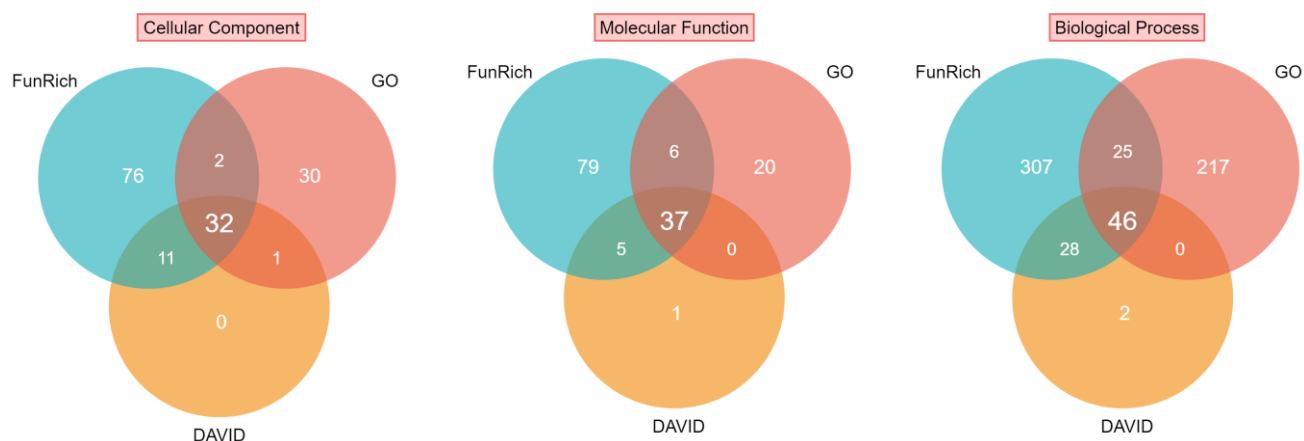


Figure 4. Visualization of a comparison of gene ontology data from Gene Ontology, FunRich, and DAVID databases. Data were compared using a Venn diagram generator (<https://www.biotoools.fr/misc/venny/>). Mutual terms identified by all databases are listed in Appendix, Table S2.

3.4. Characterization of EVs

Since UC was identified as the most effective isolation method, EV samples isolated using UC were selected for further characterization. A Western blot analysis confirmed the presence of CD9, CD63, and CD81 (Figure 5a). The chosen markers belong to the family of tetraspanins and are commonly used as EV markers. Calnexin, serving as the negative marker of EVs, was not detected in the EV samples, thus confirming the absence of cellular contamination. The size distribution of particles was determined by DLS measurement (Figure 5b). The average size of particles was 181.7 nm with a standard deviation (SD) value of 11.8 nm. The polydispersity of a sample is demonstrated as a polydispersity index (PDI). EVs are naturally heterogeneous in size; therefore, samples are usually polydisperse. In our case, the PDI was 0.214 with an SD of 0.047, indicating that we managed to isolate a fairly monodisperse population of EVs. A quantitative analysis of transmission electron microscopy (TEM) images showed that the particles had an average diameter of 72.8 nm, while the SD was 58.4 nm ($n = 37$). Larger sizes measured by DLS are due to differences in the characterization techniques' working principles. DLS values (i.e., hydrodynamic radii of particles) are determined using the Stokes-Einstein equation [47]. These values are presented as either a Z-average or cumulants mean. However, the results of DLS analysis are skewed towards larger particles. This is because the scattering intensity scales with the sixth power of the particle diameter, so larger particles disproportionately dominate the signal [47]. TEM revealed the characteristic cup-shaped morphology of EVs (Figure 5c).

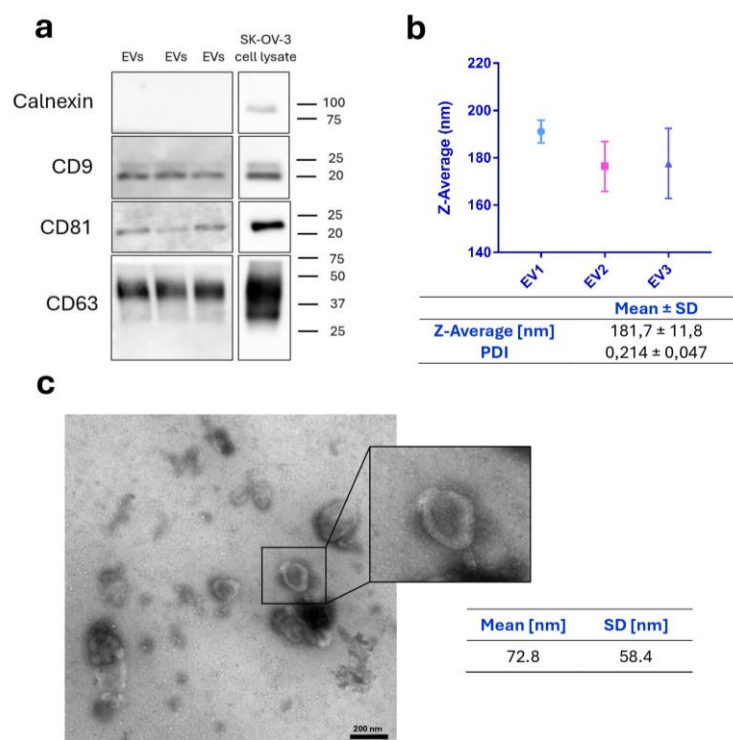


Figure 5. Characterization of EVs isolated by UC. (a) Results of Western blot analysis. (b) DLS analysis revealed the average size of EVs as 181.7 nm, the minimum size as 168.3 nm, and the maximum size as 195.9 nm. The graph visualizes measurements for each sample from the biological triplicate; the table summarizes the values for the overall measurement. The average PDI of the samples was 0.214. The detailed information for each measurement is shown in the Appendix, Figure S4a. (c) TEM micrographs show typical cup-shaped EVs: the average size of vesicles ($n = 37$) was determined to be 72.8 nm, the minimum size was 15.0 nm, and the maximum size was 238.8 nm (scale bar, 200 nm). The size distribution of EVs from the TEM is summarized in the Appendix, Figure S4b.

4. Discussion

In this study, we presented a comparison of several techniques for the isolation of EVs. Because the principles that underlie the isolation methods differ, the resulting EV protein profiles varied across the isolation techniques. The additional value of our work lies in the comprehensive report on the EV proteome of the SK-OV-3 cell line. To the best of our knowledge, no study has reported the EV proteome of the SK-OV-3 cell line isolated in parallel using five different methods.

UC proved to be the best method, as the number of isolated proteins was the highest and the ratio of significant proteins to contaminants was the most favorable. The proposed general outline of differential UC consists of multiple centrifugal steps with increasing rotational speeds for the subsequent removal of cells, cell debris, and large EVs [48]. An alternative approach may involve a filtration step [49]. In its core, the UC protocol is simple, and it allows for the handling of large volumes of samples. On the other hand, it is quite laborious and might even have damaging effects on EVs [50]. Usual obstacles are aggregated proteins in the resulting sample, lipoprotein contamination, or a low

EV count [51]. In accordance with MISEV2023 guidelines, the emphasis is on the diligent reporting of conditions in which UC was carried out since the type of rotor, centrifugal force, and time affect the overall result [52].

Ultrafiltration is easy to perform; however, it often results in clogged pores [53]. TFF, as described by Busatto et al., utilizes a mechanism that overcomes this issue [53]. In general, TFF often performs better than UC [54]. Our study showed the opposite result. The reason behind this might be the device itself. The device must be unique on the market, as even after a thorough literature search, there is no publication specifically dedicated to this product. The manufacturer's recommendation mentions multiple applications. It would probably perform better if it were used to concentrate the CCM, and the isolation step would be carried out by a different method.

Precipitation is a popular approach [55]. EV separation is usually facilitated by polyethylene glycol (PEG) [56]. The attractiveness of precipitation lies in its simplicity, low cost, high yields, and intact EVs. In contrast, the sample purity is poor due to coprecipitated protein and leftover precipitation agent [57].

Affinity-based approaches rely on the presence of specific biomarkers located on the surface of EVs [58]. This principle provides EVs of a high purity [59] at the cost of leaving many EVs in the mixture, as they do not contain the specific marker used for isolation [60]. Noteworthy results brought the idea of utilizing T-cell immunoglobulin domain and mucin domain-containing protein 4 (Tim4) to bind phosphatidylserine, a molecule abundantly present on the surface of EVs [61]. Nakai et al. found this technique superior to UC and TEI, while our results favor UC, possibly due to uneven initial CCM volumes. We excluded the wash step due to a significant EV loss, a concern also noted by Nakai et al [61].

The exoEasy Maxi kit is based on the membrane-affinity principle. The spin-column technique should not enable the co-isolation of contaminants such as plasma proteins, lipoproteins, or RNP complexes. However, the significant presence of albumin in the isolated samples suggests otherwise [62].

Briefly, every method has its advantages and limitations, as also illustrated in Table 2. Individual approaches offer different qualities. Thus, the isolation method should be selected based on the specific needs of the downstream application.

Our comparison identified UC as the most effective isolation method since UC yielded the highest number of identified proteins in our experimental setup; however, the difference may partly reflect the input volume and sample handling. Especially for certain methods (TEI, MagCapture), the starting volume was only 1 ml, which only contains a small number of EVs. Therefore, the detection of a large variety of proteins is much harder. Volumes of the collected CCM varied due to differences among methods and isolation kits, since different protocols require different amounts of the CCM to isolate the EVs. The starting volumes of the CCM are listed in Table 3.

Another possible improvement would be to allow cells to produce EVs for a longer time than 24 hours in media without FBS. However, this would expose cells to stress for a longer time, which would be reflected in the EV protein cargo.

Table 2. Comparison of isolation techniques.

Method	EVs size	Purity	Advantages	Disadvantages
Differential ultracentrifugation	30–150 nm [56]	Medium [63]	suitable for large-volume samples, simple operation, low cost, high yield [64]	time-consuming, low recovery rate, poor repeatability [65], structural damage of EVs [66], co-isolation of other non-EV components [67]
Tangential flow filtration	123 ± 11.3 nm [68]	TFF > UC [53]	high yield, time-efficient, scalable [53]	higher cost if using disposable filters [53], contamination with debris and protein [68]
Precipitation (TEI)	52.5–100 nm [69]	Low [70]	simple to perform, neutral pH, unharmed to EVs [71]	co-isolation of other non-EV components, presence of polymer in the final sample (+ problems with downstream analyses) [71]
Affinity-based (ExoEasy)	186 nm [72]	Medium [72]	easy to perform, purity [73]	lipoprotein contamination [73]
Affinity-based (MagCapture)	106 ± 4.1 nm [61]	High [61]	purity, EVs of higher quality, reproducibility [61]	cost, cannot distinguish between exosomes and microvesicles [61]

Table 3. Starting volumes of CCM for EV isolation.

Isolation method	Principle	Starting volume of CCM
UC	sedimentation	16 mL
TFF	tangential flow filtration	20 mL
TEI	precipitation	1 mL
ExoEasy	affinity	8 mL
MagCapture	affinity	1 mL

Then, our interest shifted to the characteristics of the identified common proteins. For this purpose, we used three different bioinformatic tools. The term analysis confirmed the high probability that the identified proteins originated in the EVs. According to the overlapping results from the databases, these proteins are linked to several binding activities such as ‘protein binding,’ ‘cadherin binding,’ ‘heparin binding,’ etc. The analysis of biological processes revealed a wide range of biological functions in which these proteins may be involved. Both ‘cell adhesion’ and ‘cell migration’ appeared in the common data set. Such findings may point to the changing nature of a malignant cell that undergoes the EMT process. Terms such as ‘angiogenesis’ or ‘negative regulation of apoptotic process’ may also be present due to the malignant nature of cells that the EVs were isolated from.

Each technique has its own perks and flaws. The question of how to obtain the best features and eliminate imperfections of a certain method could be solved by combining different techniques [23]. However, several issues arise even with this approach. Naturally, such a protocol would take longer. The more steps the procedure has, the bigger loss of material is going to occur. Therefore, larger input volumes are required. Additionally, the cost of material and equipment is not negligible [66].

Even though many techniques have been investigated for EV isolation, novel approaches are being explored to achieve a higher purity, yield, and reproducibility. Hydrogels present one of the many examples. They have been tested not only for EV isolation but also for detection and EV delivery. The porous structure of hydrogels allows for the accurate and non-destructive isolation of EVs from biological fluids [74]. Noteworthy results were reported by Tang et al., who succeeded in isolating EVs using a DNA-based hydrogel. The isolated EVs remained intact and were further analyzed for the diagnosis of breast cancer in serum [75]. Numerous advances in EV isolation, detection, and engineering have been made in the field of microfluidics. Microfluidic platforms manipulate particles with a high precision, thus allowing for label-free isolation with a high purity and yield. [76]

This study is only focused on EV isolation from the CCM. However, the techniques described are widely used among EV researchers and can be applied to the isolation of EVs from different sources. In addition to the CCM or blood, UC, precipitation, TFF, or affinity-based methods have been used to isolate plant or bacterial EVs. Plant EVs recently emerged as promising candidates for therapeutic developments and, in the future, may play a crucial role in the cosmetic industry and drug supplements [77]. UC is commonly used to isolate bacterial EVs. Due to the problems with purity, other approaches have been used, such as density gradient UC or SEC. Bacterial EVs are being investigated as potential alternatives to antibiotics to combat bacterial infections and for wound healing applications [78]. Even though the source of EVs may differ, so far, no standardized isolation protocol has been established. The issues with high purity and reproducibility require further investigation and development.

5. Conclusions

The isolation of EVs is still a topic with no definitive answer. The choice of a suitable isolation method depends on various factors, such as the type of biological fluid and the required input volume. One must take the working principle of a chosen technique into consideration, since different methods may produce different subtypes of EVs. Our study observation points out the importance of UC. UC has its rightful place among isolation methods; however, more and more researchers opt for different and easier approaches, such as SEC. Clinical practice requires techniques that are easy to handle and relatively quick. UC provides the best results, but the process is laborious and time-consuming. Nonetheless, it remains the gold standard.

Author contributions

Klara Mrazova: data curation, formal analysis, investigation, validation, visualization, writing—original draft, writing—review & editing; Tomas Henek: investigation; Zuzana Mihal Jurikova: investigation; Simona Koznarova: investigation, writing—original draft; Michaela Vasinova Galiova: funding acquisition, project administration, supervision; Jaromir Bacovsky: investigation, writing—original draft; Lenka Hernychova: funding acquisition, project administration, supervision, writing—review & editing; Roman Hrstka: conceptualization, funding acquisition, methodology, project administration, supervision, writing—review & editing.

Use of Generative-AI tools declaration

The authors declare they have not used Artificial Intelligence (AI) tools in the creation of this article.

Acknowledgments

This work was supported by the project National Institute for Cancer Research (Programme EXCELES, ID Project No. LX22NPO5102) - Funded by the European Union - Next Generation EU, by MH CZ - DRO (MMCI, 00209805) and by the project FCH-S-25-8807 of Ministry of Education, Youth and Sports of the Czech Republic.

Conflict of interest

The authors declare no conflict of interest in this paper.

References

1. Yang C, Robbins PD (2011) The roles of tumor-derived exosomes in cancer pathogenesis. *Clin Dev Immunol* 2011: 842849. <https://doi.org/10.1155/2011/842849>

2. Ciardiello C, Migliorino R, Leone A, et al. (2020) Large extracellular vesicles: Size matters in tumor progression. *Cytokine Growth Factor Rev* 51: 69–74. <https://doi.org/10.1016/j.cytogfr.2019.12.007>
3. Tkach M, Théry C (2016) Communication by extracellular vesicles: Where we are and where we need to go. *Cell* 164: 1226–1232. <https://doi.org/10.1016/j.cell.2016.01.043>
4. Willms E, Cabañas C, Mäger I, et al. (2018) Extracellular vesicle heterogeneity: Subpopulations, isolation techniques, and diverse functions in cancer progression. *Front Immunol* 9: 738. <https://doi.org/10.3389/fimmu.2018.00738>
5. Halicka HD, Bedner E, Darzynkiewicz Z (2020) Segregation of RNA and separate packaging of DNA and RNA in apoptotic bodies during apoptosis. *Exp Cell Res* 260: 248–256. <https://doi.org/10.1006/excr.2000.5027>
6. Chen J, Li P, Zhang T, et al. (2022) Review on strategies and technologies for exosome isolation and purification. *Front Bioeng Biotechnol* 9: 811971. <https://doi.org/10.3389/fbioe.2021.811971>
7. Stoorvogel W, Kleijmeer MJ, Geuze HJ, et al. (2002) The biogenesis and functions of exosomes. *Traffic* 3: 321–330. <https://doi.org/10.1034/j.1600-0854.2002.30502.x>
8. Booth AM, Fang Y, Fallon JK, et al. (2006) Exosomes and HIV Gag bud from endosome-like domains of the T cell plasma membrane. *J Cell Biology* 172: 923–935. <https://doi.org/10.1083/jcb.200508014>
9. Wolf P (1967) The nature and significance of platelet products in human plasma. *Br J Haematol* 13: 269–288. <https://doi.org/10.1111/j.1365-2141.1967.tb08741.x>
10. Harding C, Heuser J, Stahl P (1983) Receptor-mediated endocytosis of transferrin and of the transferrin receptor in rat reticulocytes recycling. *J Cell Biol* 97: 329–339. <https://doi.org/10.1083/jcb.97.2.329>
11. Pan BT, Johnstone RM (1983) Fate of the transferrin receptor during maturation of sheep reticulocytes in vitro: Selective externalization of the receptor. *Cell* 33: 967–978. [https://doi.org/10.1016/0092-8674\(83\)90040-5](https://doi.org/10.1016/0092-8674(83)90040-5)
12. Doyle LM, Wang MZ (2019) Overview of extracellular vesicles, their origin, composition, purpose, and methods for exosome isolation and analysis. *Cells* 8: 727. <https://doi.org/10.3390/cells8070727>
13. Valadi H, Ekström K, Bossios A, et al. (2007) Exosome-mediated transfer of mRNAs and microRNAs is a novel mechanism of genetic exchange between cells. *Nat Cell Biol* 9: 654–659. <https://doi.org/10.1038/ncb1596>
14. Skog J, Würdinger T, van Rijn S, et al. (2008) Glioblastoma microvesicles transport RNA and proteins that promote tumour growth and provide diagnostic biomarkers. *Nat Cell Biol* 10: 1470–1476. <https://doi.org/10.1038/ncb1800>
15. Hood JL, San RS, Wickline SA (2011) Exosomes released by melanoma cells prepare sentinel lymph nodes for tumor metastasis. *Cancer Res* 71: 3792–3801. <https://doi.org/10.1158/0008-5472.CAN-10-4455>
16. Sharghi-Namini S, Tan E, Ong LLS, et al. (2014) Dll4-containing exosomes induce capillary sprout retraction in a 3D microenvironment. *Sci Rep* 4: 4031. <https://doi.org/10.1038/srep04031>
17. Dilsiz N (2022) Hallmarks of exosomes. *Future Sci OA* 8: FSO764. <https://doi.org/10.2144/fsoa-2021-0102>
18. Théry C, Ostrowski M, Segura E (2009) Membrane vesicles as conveyors of immune responses. *Nat Rev Immunol* 9: 581–593. <https://doi.org/10.1038/nri2567>

19. Huang X, Yuan T, Liang M, et al. (2015) Exosomal miR-1290 and miR-375 as prognostic markers in castration-resistant prostate cancer. *Eur Urol* 67: 33–41. <https://doi.org/10.1016/j.eururo.2014.07.035>
20. Rabinowits G, Gerçel-Taylor C, Day JM, et al. (2009) Exosomal microRNA: A diagnostic marker for lung cancer. *Clin Lung Cancer* 10: 42–46. <https://doi.org/10.3816/CLC.2009.n.006>
21. Raposo G, Stoorvogel W (2013) Extracellular vesicles: Exosomes, microvesicles, and friends. *J Cell Biol* 200: 373–383. <https://doi.org/10.1083/jcb.201211138>
22. Février B, Raposo G (2004) Exosomes: Endosomal-derived vesicles shipping extracellular messages. *Curr Opin Cell Biol* 16: 415–421. <https://doi.org/10.1016/j.ceb.2004.06.003>
23. Witwer KW, Buzás EI, Bemis LT, et al. (2013) Standardization of sample collection, isolation and analysis methods in extracellular vesicle research. *J Extracell Vesicles* 2: 20360. <https://doi.org/10.3402/jev.v2i0.20360>
24. Wubbolts R, Leckie RS, Veenhuizen PTM, et al. (2003) Proteomic and biochemical analyses of human B cell-derived exosomes: Potential implications for their function and multivesicular body formation. *J Biol Chem* 278: 10963–10972. <https://doi.org/10.1074/jbc.M207550200>
25. Subra C, Laulagnier K, Perret B, et al. (2007) Exosome lipidomics unravels lipid sorting at the level of multivesicular bodies. *Biochimie* 89: 205–212. <https://doi.org/10.1016/j.biochi.2006.10.014>
26. Bellingham SA, Coleman BM, Hill AF (2012) Small RNA deep sequencing reveals a distinct miRNA signature released in exosomes from prion-infected neuronal cells. *Nucleic Acids Res* 40: 10937–10949. <https://doi.org/10.1093/nar/gks832>
27. Kitai Y, Kawasaki T, Sueyoshi T, et al. (2017) DNA-containing exosomes derived from cancer cells treated with topotecan activate a STING-dependent pathway and reinforce antitumor immunity. *J Immunol* 198: 1649–1659. <https://doi.org/10.4049/jimmunol.1601694>
28. Van Niel G, Porto-Carreiro I, Simoes S, et al. (2006) Exosomes: A common pathway for a specialized function. *J Biochem* 140: 13–21. <https://doi.org/10.1093/jb/mvj128>
29. Guo W, Gao Y, Li N, et al. (2017) Exosomes: New players in cancer (Review). *Oncol Rep* 38: 665–675. <https://doi.org/10.3892/or.2017.5714>
30. Martins TS, Vaz M, Henriques AG (2023) A review on comparative studies addressing exosome isolation methods from body fluids. *Anal Bioanal Chem* 415: 1239–1263. <https://doi.org/10.1007/s00216-022-04174-5>
31. Théry C, Witwer KW, Aikawa E, et al. (2018) Minimal information for studies of extracellular vesicles 2018 (MISEV2018): A position statement of the International Society for Extracellular Vesicles and update of the MISEV2014 guidelines. *J Extracell Vesicles* 7: 1535750. <https://doi.org/10.1080/20013078.2018.1535750>
32. Matsuzaka Y, Yashiro R (2022) Advances in purification, modification, and application of extracellular vesicles for novel clinical treatments. *Membranes* 12: 1244. <https://doi.org/10.3390/membranes12121244>
33. Li J, Lee Y, Johansson HJ, et al. (2015) Serum-free culture alters the quantity and protein composition of neuroblastoma-derived extracellular vesicles. *J Extracell Vesicles* 4: 26883. <https://doi.org/10.3402/jev.v4.26883>
34. Lehrich BM, Liang Y, Khosravi P, et al. (2018) Fetal bovine serum-derived extracellular vesicles persist within vesicle-depleted culture media. *Int J Mol Sci* 19: 3538. <https://doi.org/10.3390/ijms19113538>

35. Rolfo C, Castiglia M, Hong D, et al. (2014) Liquid biopsies in lung cancer: The new ambrosia of researchers. *BBA-Rev Cancer* 1846: 539–546. <https://doi.org/10.1016/j.bbcan.2014.10.001>
36. Crescitelli R, Lässer C, Lötvall J (2021) Isolation and characterization of extracellular vesicle subpopulations from tissues. *Nat Protoc* 16: 1548–1580. <https://doi.org/10.1038/s41596-020-00466-1>
37. Carnino JM, Lee H, Jin Y (2019) Isolation and characterization of extracellular vesicles from Broncho-Alveolar lavage fluid: A review and comparison of different methods. *Respir Res* 20: 240. <https://doi.org/10.1186/s12931-019-1210-z>
38. Gardiner C, Di Vizio D, Sahoo S, et al. (2016) Techniques used for the isolation and characterization of extracellular vesicles: Results of a worldwide survey. *J Extracell Vesicles* 5: 32945. <https://doi.org/10.3402/jev.v5.32945>
39. Royo F, Théry C, Falcón-Pérez JM, et al. (2020) Methods for separation and characterization of extracellular vesicles: Results of a worldwide survey performed by the ISEV rigor and standardization subcommittee. *Cells* 9: 1955. <https://doi.org/10.3390/cells9091955>
40. Sherman BT, Hao M, Qiu J, et al. (2022) DAVID: A web server for functional enrichment analysis and functional annotation of gene lists (2021 update). *Nucleic Acids Res* 50: W216–W221. <https://doi.org/10.1093/nar/gkac194>
41. Huang DW, Sherman BT, Lempicki RA (2009) Systematic and integrative analysis of large gene lists using DAVID bioinformatics resources. *Nat Protoc* 4: 44–57. <https://doi.org/10.1038/nprot.2008.211>
42. Ashburner M, Ball CA, Blake JA, et al. (2000) Gene ontology: Tool for the unification of biology. *Nat Genet* 25: 25–29. <https://doi.org/10.1038/75556>
43. The Gene Ontology Consortium, Aleksander SA, Balhoff J, Carbon S, et al. (2023) The gene ontology knowledgebase in 2023. *Genetics* 224: iyad031. <https://doi.org/10.1093/genetics/iyad031>
44. Thomas PD, Ebert D, Muruganujan A, et al. (2022) PANTHER: Making genome-scale phylogenetics accessible to all. *Protein Sci* 31: 8–22. <https://doi.org/10.1002/pro.4218>
45. Fonseka P, Pathan M, Chitti SV, et al. (2021). FunRich enables enrichment analysis of OMICs datasets. *J Mol Biol* 433: 166747. <https://doi.org/10.1016/j.jmb.2020.166747>
46. Chitti SV, Gummadi S, Kang T, et al. (2024) Vesiclepedia 2024: An extracellular vesicles and extracellular particles repository. *Nucleic Acids Res* 52: D1694–D1698. <https://doi.org/10.1093/nar/gkad1007>
47. Khan MA, Anand S, Deshmukh SK, et al. (2022) Determining the size distribution and integrity of extracellular vesicles by dynamic light scattering. In: *Methods in molecular biology*. New York: Humana 2413: 165–175. https://doi.org/10.1007/978-1-0716-1896-7_17
48. Szatanek R, Baran J, Siedlar M, et al. (2015) Isolation of extracellular vesicles: Determining the correct approach (Review). *Int J Mol Med* 36: 11–17. <https://doi.org/10.3892/ijmm.2015.2194>
49. Théry C, Amigorena S, Raposo G, et al. (2006) Isolation and characterization of exosomes from cell culture supernatants and biological fluids. *Curr Protoc Cell Biol* 30: 3-22. <https://doi.org/10.1002/0471143030.cb0322s30>
50. Lobb RJ, Becker M, Wen SW, et al. (2015) Optimized exosome isolation protocol for cell culture supernatant and human plasma. *J Extracell Vesicles* 4: 27031. <https://doi.org/10.3402/jev.v4.27031>

51. Brennan K, Martin K, FitzGerald SP, et al. (2020) A comparison of methods for the isolation and separation of extracellular vesicles from protein and lipid particles in human serum. *Sci Rep* 10: 1039. <https://doi.org/10.1038/s41598-020-57497-7>
52. Welsh JA, Goberdhan DCI, O'Driscoll L, et al. (2024) Minimal information for studies of extracellular vesicles (MISEV2023): From basic to advanced approaches. *J Extracell Vesicles* 13: e12404. <https://doi.org/10.1002/jev2.12404>
53. Busatto S, Vilanilam G, Ticer T, et al. (2018) Tangential flow filtration for highly efficient concentration of extracellular vesicles from large volumes of fluid. *Cells* 7: 273. <https://doi.org/10.3390/cells7120273>
54. Visan KS, Lobb RJ, Ham S, et al. (2022) Comparative analysis of tangential flow filtration and ultracentrifugation, both combined with subsequent size exclusion chromatography, for the isolation of small extracellular vesicles. *J Extracell Vesicles* 11: 12266. <https://doi.org/10.1002/jev2.12266>
55. Stam J, Bartel S, Bischoff R, et al. (2021) Isolation of extracellular vesicles with combined enrichment methods. *J Chromatogr B* 1169: 122604. <https://doi.org/10.1016/j.jchromb.2021.122604>
56. Zeringer E, Barta T, Li M, et al. (2015) Strategies for isolation of exosomes. *Cold Spring Harb Protoc* 2015: 319–323. <https://doi.org/10.1101/pdb.top074476>
57. Monguió-Tortajada M, Gálvez-Montón C, Bayes-Genis A, et al. (2019) Extracellular vesicle isolation methods: Rising impact of size-exclusion chromatography. *Cell Mol Life Sci* 76: 2369–2382. <https://doi.org/10.1007/s00018-019-03071-y>
58. Ueda K, Ishikawa N, Tatsuguchi A, et al. (2014) Antibody-coupled monolithic silica microtips for highthroughput molecular profiling of circulating exosomes. *Sci Rep* 4: 6232. <https://doi.org/10.1038/srep06232>
59. Zarovni N, Corrado A, Guazzi P, et al. (2015) Integrated isolation and quantitative analysis of exosome shuttled proteins and nucleic acids using immunocapture approaches. *Methods* 87: 46–58. <https://doi.org/10.1016/j.ymeth.2015.05.028>
60. Mizutani K, Terazawa R, Kameyama K, et al. (2014) Isolation of prostate cancer-related exosomes. *Anticancer Res* 34: 3419-3423.
61. Nakai W, Yoshida T, Diez D, et al. (2016) A novel affinity-based method for the isolation of highly purified extracellular vesicles. *Sci Rep* 6: 33935. <https://doi.org/10.1038/srep33935>
62. Stranska R, Gysbrechts L, Wouters J, et al. (2018) Comparison of membrane affinity-based method with size-exclusion chromatography for isolation of exosome-like vesicles from human plasma. *J Transl Med* 16: 1. <https://doi.org/10.1186/s12967-017-1374-6>
63. Momen-Heravi F (2017) Isolation of extracellular vesicles by ultracentrifugation. In: *Methods in molecular biology* 1660: 25–32. https://doi.org/10.1007/978-1-4939-7253-1_3
64. Jia Y, Yu L, Ma T, et al. (2022) Small extracellular vesicles isolation and separation: Current techniques, pending questions and clinical applications. *Theranostics* 12: 6548–6475. <https://doi.org/10.7150/thno.74305>
65. Lin S, Yu Z, Chen D, et al. (2020) Progress in microfluidics-based exosome separation and detection technologies for diagnostic applications. *Small* 16: 1903916. <https://doi.org/10.1002/smll.201903916>
66. Li P, Kaslan M, Lee SH, et al. (2017) Progress in exosome isolation techniques. *Theranostics* 7: 789–804. <https://doi.org/10.7150/thno.18133>

67. Jeppesen DK, Hvam ML, Primdahl-Bengtson B, et al. (2014) Comparative analysis of discrete exosome fractions obtained by differential centrifugation. *J Extracell Vesicles* 3: 25011. <https://doi.org/10.3402/jev.v3.25011>
68. Heath N, Grant L, De Oliveira TM, et al. (2018) Rapid isolation and enrichment of extracellular vesicle preparations using anion exchange chromatography. *Sci Rep* 8: 5730. <https://doi.org/10.1038/s41598-018-24163-y>
69. Xiong YH, Fan XG, Chen YY, et al. (2022) Comparison of methods of isolating extracellular vesicle microRNA from HepG2 cells for High-throughput sequencing. *Front Mol Biosci* 9: 976528. <https://doi.org/10.3389/fmolb.2022.976528>
70. Coumans FAW, Brisson AR, Buzas EI, et al. (2017) Methodological guidelines to study extracellular vesicles. *Circ Res* 120: 1632–1648. <https://doi.org/10.1161/CIRCRESAHA.117.309417>
71. Taylor DD, Shah S (2015) Methods of isolating extracellular vesicles impact down-stream analyses of their cargoes. *Methods* 87: 3–10. <https://doi.org/10.1016/j.ymeth.2015.02.019>
72. Veerman RE, Teeuwen L, Czarnewski P, et al. (2021) Molecular evaluation of five different isolation methods for extracellular vesicles reveals different clinical applicability and subcellular origin. *J Extracell Vesicles* 10: e12128. <https://doi.org/10.1002/jev2.12128>
73. Macías M, Rebmann V, Mateos B, et al. (2019) Comparison of six commercial serum exosome isolation methods suitable for clinical laboratories. Effect in cytokine analysis. *Clin Chem Lab Med* 57: 1539–1545. <https://doi.org/10.1515/cclm-2018-1297>
74. Li Y, Liu Z, Zheng Z, et al. (2025) Hydrogel empowered extracellular vesicles isolation, detection, and delivery. *Nano Today* 64: 102817. <https://doi.org/10.1016/j.nantod.2025.102817>
75. Tang J, Jia X, Li Q, et al. (2023) A DNA-based hydrogel for exosome separation and biomedical applications. *Proc Natl Acad Sci U S A* 120. <https://doi.org/10.1073/pnas.2303822120>
76. Tian F, Liu C, Deng J, et al. (2022) Microfluidic separation, detection, and engineering of extracellular vesicles for cancer diagnostics and drug delivery. *Acc Mater Res* 3: 498–510. <https://doi.org/10.1021/accountsmr.1c00276>
77. Jo HY, Kang SJ, Kim G, et al. (2025) Plant-derived extracellular vesicles: Current status and challenges for developing a new paradigm in therapeutics development. *VIEW* 6: 20240115. <https://doi.org/10.1002/VIW.20240115>
78. Shi Y, Zheng Z, Li Y, et al. (2026) Bacterial extracellular vesicles as bioactive nanocarriers for wound treatment. *Acta Pharm Sin B* 2026. In press. <https://doi.org/10.1016/j.apsb.2026.01.007>



AIMS Press

© 2026 the Author(s), licensee AIMS Press. This is an open access article distributed under the terms of the Creative Commons Attribution License (<http://creativecommons.org/licenses/by/4.0>)